Negligible Climatic Effects from the 2008 Okmok and Kasatochi Volcanic Eruptions

Ben Kravitz[1], Alan Robock[1], and Adam Bourassa[2]

[1]Department of Environmental Sciences, Rutgers University, New Brunswick, New Jersey

[2]Department of Physics and Engineering Physics, University of Saskatchewan, Saskatoon, Saskatchewan

January, 2010

Revised March, 2010

Journal of Geophysical Research – Atmospheres, in press

Ben Kravitz, Department of Environmental Sciences, Rutgers University, 14 College Farm Road, New Brunswick, NJ 08901, USA. (benkravitz@envsci.rutgers.edu) **(Corresponding Author)**

Alan Robock, Department of Environmental Sciences, Rutgers University, 14 College Farm Road, New Brunswick, NJ 08901, USA. (robock@envsci.rutgers.edu)

Adam Bourassa, Department of Physics and Engineering Physics, University of Saskatchewan, 116 Science Place, Saskatoon, SK S7N 5E2, Canada. (adam.bourassa@usask.ca)

Abstract

We used a general circulation model of Earth's climate to conduct simulations of climate response to the July 12, 2008, eruption of Okmok volcano and the August 8, 2008, eruption of Kasatochi volcano, which injected a total of 1.6 Tg of SO_2 into the Arctic upper troposphere and lower stratosphere (0.1 Tg from Okmok and 1.5 Tg from Kasatochi). For the climate model simulations, we placed all the SO_2 into the lower stratosphere. The temporal and spatial distribution of model predictions of sulfate aerosol optical depth agree with measurements made by the Optical Spectrograph and InfraRed Imaging System (OSIRIS), a Canadian satellite instrument. After accounting for differences due to different wavelengths, different sampling volumes, and an overestimate of stratospheric SO_2 loading in the model, the optical depths measured by OSIRIS are consistent with the modeled values. Although the shortwave radiative effects of the eruption are detectable in model output, perturbations in surface air temperature and precipitation were negligible, since the Okmok injection was quite small and the Kasatochi eruption was too late in the year for there to have been large radiative forcing in 2008 and was of insufficient magnitude for the sulfate aerosols to persist in the stratosphere into the following spring. We conducted further experiments with lower stratospheric injections of 3 and 5 Tg of SO_2 into the Arctic on August 8, 2008. Although the sulfate aerosol optical depth and resulting shortwave radiative forcing increase linearly with atmospheric loading of SO_2, the radiative forcing was still small due to the timing of the eruption, with little insolation by the time the sulfate aerosol cloud would form. High latitude eruptions of this size occurring in August or later in the calendar year would still be of insufficient magnitude for the sulfate aerosols to persist in the stratosphere into the following spring, and climate effects would be negligible.

1. Introduction

On July 12, 2008, Okmok Volcano (53.5°N, 168.2°W) in the Aleutian Islands erupted, injecting approximately 0.1 Tg of sulfur dioxide into the lower stratosphere at an altitude of approximately 10-16 km [Simon Carn, 2008, personal communication]. On August 8, 2008, nearby Kasatochi Volcano (52.1°N, 175.3°W) erupted, injecting an additional 1.2 to 1.5 Tg of sulfur dioxide into the lower stratosphere [A. Krueger, 2008, personal communication; *Carn*, 2008]. This eruption produced the largest stratospheric SO_2 injection since the eruptions of Mount Pinatubo and Mount Hudson in 1991 [*Carn and Krueger*, 2004].

Over the course of the next few weeks, the SO_2 oxidized to form a sulfate aerosol cloud, some of which persisted for several months following the eruptions. Large volcanic eruptions are known to have an effect on the climate system, mainly due to changes in radiative forcing that result from the production of these sulfate aerosols in the lower stratosphere [*Robock*, 2000]. Sulfate aerosols are highly efficient at backscattering shortwave radiation, effectively increasing the planetary albedo, which results in cooling of the surface and the troposphere. Also, due to absorption of shortwave and near-infrared radiation by these aerosols, the stratosphere tends to warm after a large volcanic eruption [*Stenchikov et al.*, 1998]. These changes in the thermal profile of the lower and middle atmosphere can have dynamical effects, depending upon the degree to which this profile is altered and the spatial distribution of the forcing.

To have climatic effects, a volcanic aerosol cloud must be formed in the stratosphere (as opposed to the troposphere) so that it will have a sufficient atmospheric lifetime. The atmospheric lifetime of sulfate aerosols in the troposphere is at most a few weeks [*Seinfeld and Pandis*, 2006], which is an insufficient amount of time to impact the climate. However, the atmospheric lifetime in the stratosphere for tropical injections is 1-3 years [*Budyko*, 1977], with an average *e*-folding lifetime of approximately 1 year [*Stenchikov et al.*, 1998; *Gao et al.*, 2007]. This is a sufficient amount of time to cause perturbations to the climate system on at least a seasonal scale.

The climate effects of a large eruption are best understood by studying an example of a recent large volcanic eruption that is known to have a measurable climate effect: the eruption of Mount Pinatubo. This eruption occurred in the Philippines at 15.1°N on June 15, 1991, and 20 Tg of SO_2 was injected into the stratosphere [*Bluth et al.*, 1992; *Robock*, 2002]. As a result, during the boreal summer of 1992, Northern Hemisphere continents were cooler than average by up to 2°C. This cooling also resulted in an increase in the area of Arctic sea ice [*Robock*, 2003a]. This cooler summer was bracketed by surface air temperature warming over the Northern Hemisphere continents during the boreal winters of 1991-1992 and 1992-1993. The winter warming is a dynamical response to temperature gradients produced in the lower stratosphere due to aerosol heating, ozone depletion, and reduced tropical storminess [*Robock*, 2003b]. Other dynamical effects combined to produce a positive mode of the Arctic Oscillation for the two winters following the eruption [*Stenchikov et al.*, 2002, 2004]. However, this winter warming response is only from tropical eruptions and would not be expected from the high latitude eruptions studied here [*Oman et al.*, 2005].

Volcanic eruptions have an additional climate effect, depending on the magnitude and time of year of the eruption, which is magnified when the eruption occurs at high latitudes. Large volcanic eruptions which occur at the appropriate time of year can weaken the African and Asian monsoon system. During a tropical eruption, the aerosol cloud spreads to both the Northern and Southern Hemispheres, effectively blanketing the globe, resulting in a reduction of solar flux at all latitudes [*Bluth et al.*, 1992]. Due to the land's relatively low heat capacity as

compared to that of the ocean, the decrease in temperature over land is much greater than the decrease in temperature over the ocean. This reduces the temperature gradient between the land and the ocean, and this gradient drives monsoonal precipitation. *Trenberth and Dai* [2007] showed this for the Pinatubo eruption. In a high latitude Arctic eruption, the aerosol cloud rarely travels south of 30°N, due to the large-scale circulation [*Stothers*, 1996]. This results in a decrease in solar flux over large land masses, especially Asia, while the flux into the Indian Ocean remains largely unaffected, thus magnifying the reduction of the land-ocean temperature gradient. This effect has been seen in past proxy records and climate simulations of the eruptions of Laki in 1783-1784 at 68°N [*Thordarson and Self*, 2003; *Oman et al.*, 2006a] and Katmai on June 6, 1912 at 58°N [*Oman et al.*, 2005, 2006b].

This leads to one strong motivation for this study. The eruption of Kasatochi is the first large high latitude eruption since the eruption of Katmai in 1912. However, the climate response to past high latitude eruptions, while correlated with past proxy records, still retain some inaccuracies since there was no modern, global observation system at the time of those eruptions. Conversely, the eruption of Kasatochi occurred in the presence of such an observation system, allowing us to compare model results of a high latitude eruption with very accurate instrumentation which was heretofore unavailable.

This paper has several purposes. The first is to determine whether we can detect a modeled climate impact from the eruptions of Okmok and Kasatochi. The second is to compare our simulations of aerosol formation and transport with retrievals of stratospheric aerosol optical depth from measurements made by the Optical Spectrograph and InfraRed Imaging System (OSIRIS), a Canadian instrument on the Swedish Odin satellite [*Llewellyn et al., 2004*]. The third goal is to conduct a sensitivity study to determine a threshold for how large an August high-latitude volcanic eruption must be to noticeably impact the climate.

2. Experiment

To assess the impact of the 2008 Okmok and Kasatochi eruptions on the climate system, we simulated the climate response with a coupled atmosphere-ocean general circulation model. We used ModelE, which was developed by the National Aeronautics and Space Administration Goddard Institute for Space Studies [*Schmidt et al.*, 2006]. We used the stratospheric version with 4° latitude by 5° longitude horizontal resolution and 23 vertical levels up to 80 km. It is fully coupled to a 4° latitude by 5° longitude dynamic ocean with 13 vertical levels [*Russell et al.*, 1995].

The aerosol module [*Koch et al.*, 2006] accounts for SO_2 conversion to sulfate aerosols, as well as transport and removal of the aerosols. The chemical model calculates the sulfur cycle in the stratosphere, where the conversion rate of SO_2 to sulfate is based on the respective concentrations of SO_2 and the hydroxyl radical, the latter of which is prescribed [*Oman et al.*, 2006a]. The dry aerosol effective radius is specified to be 0.25 μm, which is the value used for the simulations of the eruption of Katmai [*Oman et al.*, 2005]. The model hydrates the aerosols based on ambient humidity values according to formulas prescribed by *Tang* [1996], resulting in a distribution of hydrated aerosols with an effective radius of approximately 0.30-0.35 μm, which is consistent with the findings of *Stothers* [1997]. Radiative forcing from the aerosols is fully interactive with the atmospheric circulation. Radiative forcing in our paper is the conventional one as defined by the IPCC [*IPCC*, 2001], also called "adjusted forcing" (F_a) by *Hansen et al.* [2005]. In this calculation, the only feedback incorporated into the definition is stratospheric thermal adjustment, as illustrated in Fig. 2b of *Hansen et al.* The means by which ModelE calculates radiative forcing and fluxes are described in *Hansen et al.* [1983]. Although

Hansen et al. only discuss Model II, the predecessor to ModelE, these same methods were later updated and adapted to ModelE [*Hansen et al.*, 2005; *Schmidt et al.*, 2006].

We began with a 20-member control ensemble of 4-year runs (2007-2010), during which global greenhouse gas concentrations increased according to the Intergovernmental Panel on Climate Change's A1B scenario [*IPCC*, 2007]. The greenhouse gas concentrations at the beginning of the simulation were prescribed to be January 1, 2007 levels, and they increased to the A1B scenario's estimation of December 31, 2010 levels by the end of the simulation. Temperature trends due to model spin-up were ameliorated by utilizing initial conditions that were the result of running the model 380 years from the starting point provided by *Russell et al.* [1995]. The model was then tuned to result in a realistic globally averaged albedo of 0.3 and a zero net surface heat flux, followed by running the model for an additional 100 years. When testing the model after this period by conducting simulations of constant 2007 greenhouse gas and aerosol concentrations, no temperature trend was detected for the period 2007-2010, which is the period over which our simulations have been conducted.

To examine the effects of the volcanic eruptions, we used a 20-member ensemble of 4-year simulations covering the same time period. In these runs, greenhouse gas concentrations increased in the same manner as in the control runs. We also injected SO_2 into the grid box centered at 52°N, 172.5°W, distributed equally in the three model layers that cover an altitude of 10-16 km, in the amounts of 0.1 Tg on July 12, 2008 and 1.5 Tg on August 8, 2008. The prevailing general circulation transports the gas/aerosol cloud around the globe within a matter of weeks, so precisely prescribing the longitude of the eruption is unnecessary.

ModelE has been shown to be realistic in simulating past volcanic eruptions. Simulations of the climate response to volcanic eruptions with this model have been conducted for the eruptions of Laki in 1783-1784 [*Oman et al.*, 2006a, 2006b], Katmai in 1912 [*Oman et al.*, 2005], and Pinatubo in 1991 [*Robock et al.*, 2007]. In all of these cases, ModelE simulations agreed with observations and proxy records to such a degree that we are confident in this model's ability to predict the climatic impact of volcanic eruptions.

3. Aerosol Optical Depth

To assess the model's accuracy in reproducing the climate effects of the Okmok and Kasatochi volcanic eruptions, we must first ascertain whether the model forms, transports, and deposits the sulfate aerosols properly. Figures 1 and 2 detail the model calculations of the anomaly in spatial and temporal extent of total sulfate aerosol optical depth (mid-visible, $\lambda = 550$ nm). Anomaly is defined as the difference between the volcano ensemble and the control ensemble, thus removing the contribution to optical thickness from tropospheric sulfate aerosols. Therefore, we shall henceforth refer to these plots as stratospheric sulfate aerosol optical depth. We see that the largest anomaly of approximately 0.1 in Figure 1 occurs in September, 2008, which is consistent with our knowledge of the rate of conversion of SO_2 to sulfate aerosols. The aerosol cloud rarely passes south of 30°N, which is consistent with *Stothers* [1996]. Nearly all of the anomalies in aerosol optical depth are below measurable levels, defined for the model results to be an optical depth of 0.01, by February, 2009. *Sioris et al.* [submitted] similarly found that the stratospheric aerosol layer persisted through March, 2009. For comparison, Table 1 describes values obtained from ModelE simulations of other large volcanic eruptions, as conducted by *Oman et al.* [2006a]. Radiative forcing due to the sulfate aerosols ceases to be measurable, defined for the model results as below 0.5 W m^{-2}, by early winter. We compared these model results with measurements obtained from OSIRIS. Launched in 2001 and still currently operational, OSIRIS measures the vertical profile of limb scattered sunlight spectra.

Previous work has demonstrated the capability of retrieving information about the vertical distribution of stratospheric aerosol from limb scatter measurements [*Bourassa et al., 2007*, *2008a*; *Rault and Loughman, 2007*; *Tukiainen et al., 2008*].

For this study, vertical profiles of stratospheric aerosol extinction were retrieved from the OSIRIS measurements at a wavelength of 750 nm using the SASKTRAN forward model [*Bourassa et al., 2008b*]. Our climate model results of the spatial and temporal distribution of the stratospheric aerosol anomaly are quite similar to the OSIRIS retrievals, which are shown in Figure 3. Scattered sunlight spectra are obtained by OSIRIS at high latitudes only in the summer, as the Sun must be above the horizon at the observation point. Thus full coverage of the Northern Hemisphere is possible only until October and resumes in March. Figure 3 shows the measured aerosol optical depth from July until November, at which point OSIRIS sampling extends only to mid-latitudes. In agreement with the model results, the largest enhancement in the optical depth, approximately a factor of 3 beyond the background levels measured in July, occurred in September. Also like the model results, the measurements show that the majority of the volcanic aerosol remained at latitudes north of 30°N. However, there is a detectable enhancement in the OSIRIS measured optical depth that extends into the tropics, although this enhancement is at values well below the threshold for statistical significance in the model results. Analysis of the OSIRIS observations for March, 2009 does not show any significant enhancement beyond the background levels measured in July, 2008, confirming the model result that most of the volcanic aerosol cloud has decayed by February.

The raw optical depths measured by OSIRIS are roughly an order of magnitude smaller than those predicted by the model. However, a direct comparison between the measured and modeled optical depths is somewhat difficult. First, the modeled and measured results are at different wavelengths. In ModelE, the wavelength dependence of the optical depths in this region follows an Angstrom exponent relation. The radiative transfer code used in the model calculates an Angstrom exponent of approximately 0.63 for the effective radii of concern in this experiment, yielding a 20% difference in aerosol optical depth at 750 nm when compared to aerosol optical depth calculated at 550 nm (*i.e.*, $\tau(750)/\tau(550) \approx 0.8$). *Schuster et al.* [2006] and *Eck et al.* [1999] have measured Angstrom exponents of this value to be consistent with the particle sizes that we have assumed in our simulations.

Also, the OSIRIS measurements are used to retrieve vertical profiles of the aerosol extinction, which are then integrated vertically to obtain optical depth. For each profile, the integration is performed from the tropopause to 40 km altitude, where the tropopause is defined by the 380 K level of potential temperature. This lower bound is necessary so as not to attempt to retrieve extinction from scattered signal that may be from particles that are not stratospheric sulfate, such as clouds and dust. Using this lower bound eliminates aerosols from measurement that are contained between this lower bound and the true thermal tropopause, leading to an underestimation of aerosol optical depth in the OSIRIS retrievals. Using the model output, we estimated the effect this would have on this discrepancy in aerosol optical depth (Figure 4). When averaged over the Northern Hemisphere, we calculated that using the $\theta = 380$ K line as the lower limit results in approximately 92% of the optical depth that would result from using the thermal tropopause as the lower limit. However, since this is an average, some spatial results may differ from this value. Indeed, Figure 4 shows a large spatial difference between the modeled aerosol optical depth when using a different definition of the lower limit for calculations.

One more explanation for the discrepancy is a possible systematic error in OSIRIS due to the assumed particle size in the forward radiative transfer model. However, this error is estimated to be no more than 20% of retrieved optical depth.

A further, likely reason for this discrepancy is due to an overestimation of aerosol loading in the model. In conducting the climate model simulations, we specified an SO_2 injection of 1.5 Tg into the Arctic lower stratosphere due to Kasatochi. However, the measured value possibly varied from this amount. Arlin Krueger [personal communication, 2008] estimated the atmospheric loading due to Kasatochi was between 1.2 and 1.5 Tg (for an Okmok + Kasatochi total of 1.3 to 1.6 Tg), which could result in retrievals up to 25% lower values than modeled aerosol optical depth. Similarly, *Prata et al.* [submitted] estimate the loading due to Kasatochi to be 1.2 Tg, but they estimate the loading from Okmok to be 0.3 Tg of SO_2. We also could have underestimated the SO_2 loading, as *Karagulian et al.* [submitted] estimate the loading due to Kasatochi to be over 1.7 Tg, and *Yang et al.* [submitted] estimate it to be as much as 2.0 Tg. Giving a wide possible range, *Corradini et al*. [submitted] state that the total mass of SO_2 due to Kasatochi varies between 0.5 and 2.7 Tg, depending on the instrument used to evaluate this quantity. They also state that the loading from Okmok was between 0.1 and 0.3 Tg of SO_2. In the face of this wide range, for the purposes of calculations, we choose to assume the actual loading was between 0 and 25% lower than the modeled values, as in the estimates by *Krueger*.

Moreover, measurements from *Kristiansen et al.* [2009] show that approximately 60% of the SO_2 was injected into the stratosphere, with the rest being injected into the troposphere. Since sulfate aerosols have a much shorter atmospheric lifetime in the troposphere, these aerosols would have been removed from the atmosphere by September, 2008 instead of remaining in the stratosphere as they do in the model. From these two sources of error, given the assumptions we made about the initial SO_2 loading, the aerosol optical depth retrievals could be as little as 48% of the modeled aerosol optical depths.

Compounding these two points is an assumption implicitly made in the modeling experiment, in that the stratospheric aerosol layer due to the volcanic eruption was composed entirely of sulfate, which was the result of complete conversion of the SO_2 into sulfate aerosols. However, *Schmale et al.* [submitted] measured the volcanic aerosol layer and found that only 71% of it was sulfate, and 21% was composed of carbonaceous material. Moreover, they found that even after 3 months, not all of the SO_2 had been converted to sulfate, whereas the model's conversion rate dictated that nearly all of the SO_2 had been converted after one month. Therefore, it is again likely that the modeling experiment overestimated the amount of sulfate aerosol. However, we do not include this potential source of error in our calculations, as we do not have enough information to properly quantify it.

Some additional possible sources of discrepancy are those that affect the mean removal rate in the real world but may not be well represented in the model. Some examples include an inaccurate representation of the sedimentation rate of the aerosols, the phase of the QBO and its effects on the removal efficiency, and the phase and magnitude of tropical modes. However, we are unable to quantify these sources, so we choose not to discuss them further.

Tabulating all of these quantifiable sources of error and accounting for uncertainties, we can expect OSIRIS retrievals to be approximately 7.0 to 44.2 percent of the modeled values, leading us to conclude that the model results are consistent with the values obtained by OSIRIS. However, these percentages were obtained by assuming that a difference in the bottom boundary of the aerosol layer results in 92% of the values that would otherwise be obtained, which may not be accurate for a given point due to spatial and temporal variations. Figure 5 shows a more

detailed spatial analysis of the minimum and maximum discrepancy between the OSIRIS retrievals and the model results. However, if we account for all possible discrepancies, the modeled results are still larger than the OSIRIS retrievals by approximately a factor of 2 to 3. Further investigation and explanation is needed as to why the modeled results do not completely agree with the results from OSIRIS.

To further investigate the discrepancy between modeled and OSIRIS-observed optical depths, we tried to obtain additional observations. The only sources of data we were able to obtain are two Raman LIDAR observation systems, one operated by Dalhousie University in Halifax, Nova Scotia (44.64°N, 63.59°W), and one in Leipzig, Germany (51.4°N, 12.4°E), which can provide us with single point comparisons. The Dalhousie LIDAR operates at a wavelength of 532 nm [*Bitar et al.*, submitted], and the Leipzig LIDAR operates at wavelengths of 355 and 1064 nm [*Mattis et al.*, submitted].

For their calculations, *Bitar et al.* assumed an extinction-to-backscatter ratio of 40 sr, which is the approximate midpoint between background stratospheric aerosol levels (~20 sr) and strong stratospheric loading after a major volcanic eruption, which is approximately 60 sr. To eliminate measurement contamination from cirrus clouds, they calculated aerosol optical depth for altitudes between 15 and 19 km, which roughly corresponds to using the 380 K potential temperature line as their base for measurements, similar to OSIRIS.

The results from the Dalhousie LIDAR [*Bitar et al.*, submitted] are of the same order of magnitude as the OSIRIS retrievals, with a maximum value of τ=0.008 in September, 2008 and an average from August through October of approximately τ=0.003. However, the values do not exactly agree with the average values obtained by OSIRIS. One possible source for the discrepancy could be the location of the aerosol plume. Spatial measurements from OSIRIS [*Bourassa et al.*, submitted] show aerosol optical depth over Halifax from September, 2008 through November, 2008 is lower than the peak values in the Northern Hemisphere. This appears to be due to the edge of the aerosol plume passing over Halifax, as opposed to the regions of greatest optical depth. Also, although the θ = 380 K line roughly corresponds to 15 km in altitude, this correspondence is not exact. Finally, the estimation of the extinction-to-backscatter ratio could also be slightly incorrect, resulting in a maximum error of 40% of the retrieved values, although the actual error is probably significantly less.

The Leipzig LIDAR [*Mattis et al.*, submitted] similarly assumes a backscatter ratio of 30-50 sr at 532 nm for a stratospheric aerosol layer, which they measured from summer, 2008 through the end of August, 2009. Over this period, they found that the optical depth of stratospheric aerosols ranged between 0.004 and 0.025 at 532 nm. The value measured on August 21, 2008 was 0.016 at 532 nm, which, although lower than the model results over Europe by approximately a factor of 2, is of the same order of magnitude. They also estimate the aerosol effective radius to be 0.1-0.2 μm and the Angstrom exponent for these aerosols to be 1.0-2.0. From these measurements, it appears we overestimated the aerosol size in our modeling experiments. Given this range of Angstrom exponents, the optical depth at 750 nm could be between 53 and 73% of the optical depth at 550 nm, instead of the 80% we calculated above, which could further explain the discrepancy between the modeling results and the OSIRIS retrievals.

We would like to have more data sources to compare with our results, furthering the validation of OSIRIS and the model, but the current observation systems in deployment cannot provide us with additional information. This comparison of data sources with models, as well as

the abundant potential sources of error therein, serves to highlight the need for improvement in our aerosol monitoring capabilities.

4. Model Results of Climate Impact

Figure 6 shows zonally averaged anomalies in surface air temperature and precipitation that result from the eruptions. Almost no anomalies shown are statistically significant at a 95% confidence level as calculated using a Student's t-test. Therefore, any anomaly in these two fields that results from the volcanic eruptions cannot be distinguished from weather noise and natural variability. This is true in spite of the above results that our model may have overestimated the radiative forcing from the volcanic eruptions. We further analyzed other variables (not pictured) to assess changes in atmospheric circulation and a potential forcing of the Arctic Oscillation, but we did not find any statistically significant results.

Figure 7 more carefully analyzes monsoonal precipitation by examining spatial regions around the three large areas of summer monsoonal precipitation: India, the Sahel, and East Asia. It also shows averages over the months of the summer monsoon (JJAS) for 2008 and 2009. Examining each monsoon region, we notice a slightly wet summer over India during 2008. However, only a very small part of this anomaly is statistically significant, so we conclude that it is largely noise and not a result of the volcanic eruption. The Sahel and East Asia regions show almost no significant anomalies in monsoonal precipitation.

5. Discussion

The results show that the eruptions of Okmok and Kasatochi had a negligible impact on the climate system. To understand this, we examine the magnitude, time of year, and latitude of the eruptions.

Comparison to simulations of past volcanic eruptions shows a direct correlation between the amount of SO_2 loading and the resultant summer cooling. According to *Oman et al.* [2005], the eruption of Katmai, which, at 5 Tg of stratospheric SO_2, is the smallest past eruption for which we have previous simulation results, resulted in a maximum point value (JJA average over a grid box) cooling of 1 to 1.5°C. Therefore, we would expect cooling due to Okmok and Kasatochi to be even smaller, since the magnitude of these eruptions were clearly smaller than that of the eruption of Katmai. However, the summer variability in surface air temperature has point values also within this range, so even if the volcanic eruption did result in cooling during the summer, we are unable to detect it.

Another reason Kasatochi would not be expected to have a climatic impact is that it erupted relatively late in the year. The bulk of the SO_2 would be converted to sulfate aerosols after about one month, which means the radiative effects due to the aerosols would begin in September, as can be seen in Figure 2. At high latitudes, the amount of insolation in September is greatly reduced from its value in the summer and is rapidly decreasing. Since backscatter is the primary means by which volcanic eruptions have a climatic impact, the effects of the eruption of Kasatochi are strongly damped compared to what they would be had it erupted earlier in the summer. Moreover, monsoonal precipitation generally lasts from June to September. Since cooling of the land would most likely not even begin until September, the eruption essentially “missed its chance” to reduce 2008 monsoonal precipitation.

Compounding these effects is that the lifetime of stratospheric aerosols is shorter for high latitude eruptions than for tropical eruptions. Large-scale subsidence during the polar winter is responsible for removal of a large amount of volcanic sulfate aerosol [e.g., *Hamill et al.*, 1997], and much of the stratospheric lifetime is due to transport of the aerosols from low to high latitudes. Therefore, since the aerosols begin at high latitudes, the atmospheric lifetime would be

expected to be less than the usual 1-3 years. This is confirmed by the analysis of aerosol optical depth, which shows the aerosol cloud from the volcanic eruption being depleted within 6 months, as is illustrated in Figures 1, 2, and 3. *Robock et al.* [2008] used this model to calculate aerosol lifetime for a geoengineering experiment involving Arctic injections of SO_2, which bears many similarities to a high latitude volcanic eruption. They found that the *e*-folding lifetime of the sulfate aerosols is approximately 4 months in the boreal summer and 2 months in the boreal winter, which is consistent with our results.

6. Sensitivity of the Climate to Volcanic Eruptions

Throughout this paper, we have discussed the climate effects of large volcanic eruptions. However, we have, up to this point, neglected to discuss what is meant by "large." We therefore began the initial stages of a study that could determine the threshold for which the magnitude of a volcanic eruption is sufficient to produce a measurable climate response.

We used two additional ensembles of 4-year simulations covering the years 2007-2010, run with the same rate of increase of greenhouse gases as in the previous experiment. The first of these ensemble members, consisting of 20 model runs, also involved an injection of SO_2 into the grid box centered at 52°N, 172.5°W, distributed through an altitude of 10-16 km, but in the amount of 3 Tg on August 8, 2008. The second ensemble member consisted of 20 runs involving an injection of 5 Tg of SO_2. For the control case, we used the same 20 ensemble members for both the 3 Tg injection and the 5 Tg injection. The purpose of these new runs is to determine whether an increase in the magnitude of the eruption will result in a measurable climate response.

Figure 8 shows the results of this experiment by comparing aerosol optical depth and the resulting clear sky shortwave radiative forcing at the surface due to the sulfate aerosols. Both aerosol optical depth and shortwave forcing appear to increase linearly with atmospheric loading of SO_2. However, in all three experiments, none of the aerosols, nor the resulting radiative forcing, appear to persist past February, 2009. Therefore, we would not expect any of these simulations of larger volcanic eruptions to have noticeable impacts upon temperature and precipitation, and indeed, the further analysis we performed (not pictured) revealed this to be the case, despite the large radiative forcing exceeding -6 W m^{-2} between 50°N and 60°N in September, 2008 in the experiment involving a 5 Tg injection of SO_2. This does not contradict the results of *Oman et al.* [2005], since their results were just above the level of detectability above statistical noise, and although we are using the same model as was used by *Oman et al.*, some of the specifications under which we ran the model are slightly different, which could explain the different results.

Further work on this topic could include eruptions that are earlier in the year so the resultant aerosol cloud would exist during daylight months, such as the eruption of Sarychev volcano on June 12, 2009. Also, the magnitude of an August eruption could be increased to determine whether the aerosol loading could be made sufficient enough that it would persist into the following spring.

7. Relevance to Geoengineering

The study of volcanic eruptions, as well as the sensitivity study we described earlier, are particularly relevant to the topic of geoengineering with stratospheric sulfate aerosols, an idea which has recently gained renewed interest. Inspired by volcanic eruptions, this idea involves the deliberate loading of the stratosphere with sulfate aerosols in order to replicate the role of a large volcanic eruption in lowering global average temperature [*Budyko*, 1974, 1977; *Dickinson*, 1996; *Crutzen*, 2006].

Although this topic has been given increased attention in recent years, including a review paper by *Rasch et al.* [2008], certain crucial research is currently lacking. Specifically, a systematic study of various amounts of loading at different times of year and at different latitudes has not been conducted. The experiments conducted in this paper have shown that, at least as far as the experiments were taken, the magnitude of a single sulfur injection is less important than the time of year the injection occurs. Although geoengineering would involve a continuous injection of sulfur, allowing aerosols to accumulate whereas they would dissipate under a single injection, this lesson still holds true.

Also, assuming the injection occurs in time for a more effective summer radiative impact, differences in the amount and latitude of the injection can result in radically different climate impacts, not only in terms of the range of temperatures to which global average temperature can be cooled, but also the degree to which the African and Asian monsoon system is disrupted. Therefore, expanding the sensitivity study included in this paper will not only further the knowledge of the climatic impact of future volcanic eruptions, but also other potentially relevant scientific questions with future political implications, such as geoengineering.

Along these lines, *Robock et al.* [2008] and *Caldeira and Wood* [2008] have investigated limiting geoengineering with stratospheric sulfate aerosols to the Arctic. This idea has several potential advantages, including needing a reduced amount of sulfate aerosols as compared to a tropical injection, since the aerosols would only be effective during the sunlit months. Sensitivity studies of high latitude volcanic eruptions can be useful in determining the magnitude and time of year of the injection of aerosol precursors in order to produce the desired amount of climate change with the fewest negative consequences. However, there remain many reasons why geoengineering may be a bad idea [*Robock et al.*, 2009], which such a study would be incapable of addressing.

8. Conclusions

ModelE is able to provide realistic predictions regarding sulfate aerosol production and climate response to large volcanic eruptions. However, model results show sulfate aerosol optical depth values that are larger than retrieved observations. Although we have thought of several possible reasons for this discrepancy, further investigation is warranted to completely determine the cause. Regardless, both the modeled values and the retrieved values result in an insufficient amount of sulfate aerosol to significantly impact the climate.

The sensitivity study has shown that, as modeled by GISS ModelE, a high latitude volcanic eruption in August which injects 5 Tg or less of sulfur dioxide into the atmosphere is not likely to cause noticeable climatic effects. Further work could include similar magnitudes with injection earlier in the summer, such as in the June 12, 2009 volcanic eruption of Sarychev. The results show that the time of year of a high latitude eruption would have a greater impact on climate effects than the amount of the injection.

Comparison of our model simulations of the formation and distribution of stratospheric aerosols to actual observations has been very difficult, due to the lack of such observations. As pointed out by *Robock et al.* [2009], there used to be a much better observing system for stratospheric aerosols, and it has disappeared. After the 1991 Pinatubo eruption, observations with the Stratospheric Aerosol and Gas Experiment II (SAGE II) instrument on the Earth Radiation Budget Satellite [*Russell and McCormick*, 1989] showed how the aerosols spread. Right now, the only limb-scanner in orbit with the capability of observing stratospheric aerosols is OSIRIS. A SAGE III flew from 2002 to 2006, and there was no follow-on mission. Certainly,

a dedicated observational program is needed now to observe future volcanic eruptions and to monitor any future geoengineering experiments.

Acknowledgments. We thank Simon Carn and Arlin Krueger for providing estimates of volcanic emissions, Luke Oman for his help with setting up and running the model, Georgiy Stenchikov for his comments during analysis, and Lubna Bitar for providing LIDAR data and for very valuable comments during the writing of this manuscript. We also thank the reviewers and editor Steve Ghan for their helpful comments and suggestions for references. Model development and computer time at Goddard Institute for Space Studies are supported by National Aeronautics and Space Administration climate modeling grants. This work is supported by NSF grant ATM-0730452.

References

Bitar, L., T. J. Duck, N. I. Kristiansen, A. Stohl, and S. Beauchamp (2010), Lidar observations of Kasatochi volcano aerosols in the troposphere and stratosphere, *J. Geophys. Res.*, special issue, submitted.

Bluth, G. J. S., S. D. Doiron, A. J. Krueger, L. S. Walter, and C. C. Schnetzler (1992), Global tracking of the SO_2 clouds from the June 1991 Mount Pinatubo eruptions, *Geophys. Res. Lett.*, *19*, 151-154.

Bourassa, A. E., D. A. Degenstein, R. L. Gattinger, and E. J. Llewellyn (2007), Stratospheric aerosol retrieval with OSIRIS limb scatter measurements, *J. Geophys. Res.*, *112*, D10217, doi:10.1029/2006JD008079.

Bourassa, A. E., D. A. Degenstein, and E. J. Llewellyn (2008a), Retrieval of stratospheric aerosol size information from OSIRIS limb scattered sunlight spectra, *Atmos. Chem. Phys.*, *8*, 6375-6380.

Bourassa, A. E., D. A. Degenstein, and E. J. Llewellyn (2008b), SASKTRAN: A spherical geometry radiative transfer code for efficient estimation of limb scattered sunlight, J. *Quant. Spectros. Radiat. Trans*., *109*, 52-73.

Bourassa, A. E., D. A. Degenstein, B. J. Elash, and E. J. Llewellyn (2010), Evolution of the stratospheric aerosol enhancement following the Kasatochi eruption: Odin-OSIRIS measurements, *J. Geophys. Res.*, special issue, submitted.

Budyko, M. I. (1974), *Climate and Life* (Academic Press, New York, NY), 508 pp.

Budyko, M. I. (1977), *Climatic Changes* (American Geophysical Union, Washington, DC), 261 pp.

Caldeira, K. and L. Wood (2008), Global and Arctic climate engineering: Numerical model studies, *Phil. Trans. R. Soc. A*, 366, 1882, 4039-4056, doi: 10.1098/rsta.2008.0132.

Carn, S. (2008), Sulfur dioxide cloud from Aleutians' Kasatochi volcano, NASA Earth Observatory, http://earthobservatory.nasa.gov/images/imagerecords/8000/8998/kasatochi_OMI_2008aug11_lrg.jpg.

Carn, S. and A. Krueger (2004), TOMS Volcanic Emissions Group, http://toms.umbc.edu/Images/Mainpage/toms_so2chart_color.jpg.

Corradini, S., L. Merucci, A. J. Prata, and A. Piscini (2010), Volcanic ash and SO_2 in the Kasatochi and Okmok eruptions: Retrievals from different IR satellite sensors, *J. Geophys. Res*., special issue, submitted.

Crutzen, P. (2006), Albedo enhancement by stratospheric sulfur injections: A contribution to resolve a policy dilemma? *Climatic Change*, *77*, 211-219.

Dickinson, R. E. (1996), Climate engineering: A review of aerosol approaches to changing the global energy balance, *Climatic Change*, *33*, 279-290.

Eck, T. F., B. N. Holben, J. S. Reid, O. Dubovik, A. Smirnov, N. T. O'Neill, I. Slutsker, and S. Kinne (1999), Wavelength dependence of the optical depth of biomass burning, urban, and desert dust aerosols, *J. Geophys. Res.*, *104*(D24), 31333-31349, doi:10.1029/1999JD900923.

Gao, C., L. Oman, A. Robock, and G. L. Stenchikov (2007), Atmospheric volcanic loading derived from bipolar ice cores accounting for the spatial distribution of volcanic deposition, *J. Geophys. Res.*, *112*, D09109, doi:10.1029/2006JD007461.

Hamill, P., E. J. Jensen, P. B. Russell, and J. J. Bauman (1997), The life cycle of stratospheric aerosol particles, *Bull. Amer. Meteor. Soc.*, *78*, 1395–1410, doi:10.1175/1520-0477(1997)078<1395:TLCOSA>2.0.CO;2.

Hansen, J., et al. (1983), Efficient three-dimensional global models for climate studies: Models I and II, *M. Weather Rev.*, *111*, 609-662, doi:10.1175/1520-0493(1983)111<0609:ETDGMF>2.0.CO;2.

Hansen, J., et al. (2005), Efficacy of climate forcings, *J. Geophys. Res.*, *110*, D18104, doi:10.1029/2005JD005776.

IPCC (2001), *Climate Change 2001: The Scientific Basis*. Contribution of Working Group I to 1006 the Third Assessment Report of the Intergovernmental Panel on Climate Change, Houghton, J. T., Y. Ding, D. J. Griggs, M. Noguer, P. J. van der Linden, X. Dai, K. Maskell, and C.A. Johnson, Eds., (Cambridge University Press, Cambridge, United Kingdom and New York, NY, USA), 881 pp.

IPCC (2007), *Climate Change 2007: The Physical Science Basis. Contribution of Working Group I to the Fourth Assessment Report of the Intergovernmental Panel on Climate Change*, S. Solomon, D. Qin, M. Manning, Z. Chen, M. Marquis, K. B. Averyt, M. Tignor and H. L. Miller, Eds., (Cambridge University Press, Cambridge, United Kingdom and New York, NY, USA), 996 pp.

Karagulian, F., L. Clarisse, C. Clerbaux, A. J. Prata, D. Hurtmans, and P. F. Coheur (2010), Detection of volcanic SO_2, ash and H_2SO_4 using the IASI sounder, *J. Geophys. Res.*, special issue, submitted.

Koch, D., G. A. Schmidt, and C. V. Field (2006), Sulfur, sea salt, and radionuclide aerosols in GISS ModelE, *J. Geophys. Res.*, *111*, D06206, doi:10.1029/2004JD005550.

Kristiansen, N. I., A. Stohl, A. J. Prata, A. Richter, S. Eckhardt, P. Seibert, A. Hoffmann, C. Ritter, L. Bitar, T. Duck, and K. Stebel (2010), Remote sensing and inverse transport modeling of the Kasatochi eruption SO_2 cloud, *J. Geophys. Res.*, submitted.

Llewellyn, E. J., et al. (2004), The OSIRIS instrument on the Odin spacecraft, *Can. J. Phys.*, 82, 411-422.

Mattis, I., P. Seifert, D. Müller, M. Tesche, A. Hiebsch, T. Kanitz, J. Schmidt, F. Finger, U. Wandinger, and A. Ansmann (2010), Volcanic aerosol layers observed with multiwavelength Raman lidar over central Europe in 2008-2009, *J. Geophys. Res.*, submitted.

Oman, L., A. Robock, G. L. Stenchikov, G. A. Schmidt, and R. Ruedy (2005), Climatic response to high-latitude volcanic eruptions, *J. Geophys. Res.*, *110*, D13103, doi:10.1029/2004JD005487.

Oman, L., A. Robock, G. L. Stenchikov, T. Thordarson, D. Koch, D. T. Shindell, and C. Gao (2006a), Modeling the distribution of the volcanic aerosol cloud from the 1783-1784 Laki eruption, *J. Geophys. Res.*, *111*, D12209, doi:10.1029/2005JD006899.

Oman, L., A. Robock, G. L. Stenchikov, and T. Thordarson (2006b), High-latitude eruptions cast shadow over the African monsoon and the flow of the Nile, *Geophys. Res. Lett.*, *33*, L18711, doi:10.1029/2006GL027665.

Prata, A. J., G. Gangale, L. Clarisse, and F. Karagulian (2010), Ash and sulphur dioxide in the 2008 eruptions of Okmok and Kasatochi: Insights from high spectral resolution satellite measurements, *J. Geophys. Res.*, special issue, submitted.

Rasch, P. J., et al. (2008), An overview of geoengineering of climate using stratospheric sulphate aerosols, *Phil. Trans. Royal Soc. A.*, *366*, 4007-4037, doi:10.1098/rsta.2008.0131.

Rault, D., and R. Loughman (2007), Stratospheric and upper tropospheric aerosol retrieval from limb scatter signals, *Proc. SPIE*, 6745, doi:10.1117/12.737325.

Robock, A. (2000), Volcanic eruptions and climate, *Rev. Geophys.*, *38*, 191-219.

Robock, A. (2002), The climatic aftermath, *Science*, *295*, 1242-1244.

Robock, A. (2003a), Introduction: Mount Pinatubo as a test of climate feedback mechanisms, in *Volcanism and the Earth's Atmosphere*, A. Robock and C. Oppenheimer, Eds., (American Geophysical Union, Washington, DC), 1-8, doi:10.1029/139GM01.

Robock, A. (2003b), Volcanoes: Role in climate, in *Encyclopedia of Atmospheric Sciences*, J. Holton, J. A. Curry, and J. Pyle, Eds., (Academic Press, London), 2494-2500, 10.1006/rwas.2002.0169.

Robock, A. T. Adams, M. Moore, L. Oman, and G. Stenchikov (2007), Southern hemisphere atmospheric circulation effects of the 1991 Mount Pinatubo eruption, *Geophys. Res. Lett.*, *34*, L23710, doi:10.1029/2007GL031403.

Robock, A., L. Oman, and G. Stenchikov (2008), Regional climate responses to geoengineering with tropical and Arctic SO_2 injections, *J. Geophys. Res.*, *113*, D16101, doi:10.1029/2008JD010050.

Robock, A., A. Marquardt, B. Kravitz, and G. Stenchikov (2009), Benefits, risks, and costs of stratospheric geoengineering, *Geophys. Res. Lett.*, *36*, L19703, doi:10.1029/2009GL039209.

Russell, G. L., J. R. Miller, and D. Rind (1995), A coupled atmosphere-ocean model for transient climate change, *Atmos.-Ocean*, *33*, 683-730.

Russell, P. B. and M. P. McCormick (1989), SAGE II aerosol data validation and initial data use: An introduction and overview, *J. Geophys. Res.*, *94*(D6), 8335-8338.

Schmale, J., J. Schneider, T. Jurkat, C. Voigt, H. Eichler, M. Rautenhaus, M. Lichtenstern, H. Schlager, G. Ancellet, F. Arnold, M. Gerding, I. Mattis, M. Wendisch, and S. Borrmann (2010), Aerosol layers from the 2008 eruptions of Mt. Okmok and Mt. Kasatochi: In-situ UT/LS measurements of sulfate and organics over Europe, *J. Geophys. Res.*, special issue, submitted.

Schmidt, G. A., et al. (2006), Present day atmospheric simulations using GISS ModelE: Comparison to in situ, satellite and reanalysis data, *J. Climate*, *19*, 153-192.

Schuster, G. L. , O. Dubovik, and B. N. Holben (2006), Angstrom exponent and bimodal aerosol size distributions, *J. Geophys. Res.*, *111*, D07207, doi:10.1029/2005JD006328.

Seinfeld, J. H. and S. N. Pandis (2006), *Atmospheric Chemistry and Physics: From Air Pollution to Climate Change* (John Wiley and Sons, Hoboken, NJ), 1203 pp.

Sioris, C. E., C. D. Boone, P. F. Bernath, J. Zou, and C. A. McLinden (2010), ACE observations of aerosol injected into the stratosphere from the Kasatochi volcanic eruption, *J. Geophys. Res.*, submitted.

Stenchikov, G. L., I. Kirchner, A. Robock, H.-F. Graf, J. C. Antuña, R. G. Grainger, A. Lambert, and L. Thomason (1998), Radiative forcing from the 1991 Mount Pinatubo volcanic eruption, *J. Geophys. Res.*, *103*, 13837-13857, doi:10.1029/98JD00693.

Stenchikov, G., A. Robock, V. Ramaswamy, M. D. Schwarzkopf, K. Hamilton, and S. Ramachandran (2002), Arctic Oscillation response to the 1991 Mount Pinatubo eruption: Effects of volcanic aerosols and ozone depletion. *J. Geophys. Res.*, *107(D24)*, 4803, doi:10.1029/2002JD002090.

Stenchikov, G., K. Hamilton, A. Robock, V. Ramaswamy, and M. D. Schwarzkopf (2004), Arctic Oscillation response to the 1991 Pinatubo eruption in the SKYHI GCM with a realistic Quasi-Biennial Oscillation. *J. Geophys. Res.*, *109*, D03112, doi:10.1029/2003JD003699.

Stothers, R. B. (1996), Major optical depth perturbations to the stratosphere from volcanic eruptions: Pyrheliometric period, 1881-1960, *J. Geophys. Res.*, *101*, 3901-3920.

Stothers, R. B. (1997), Stratospheric aerosol clouds due to very large volcanic eruptions of the early twentieth century: Effective particle sizes and conversion from pyrheliometric to visual optical depth, *J. Geophys. Res.*, *102*(D5), 6143-6151.

Tang, I. N. (1996), Chemical and size effects of hygroscopic aerosols on light scattering coefficients, *J. Geophys. Res.*, *101*, D14, 19245-19250.

Thordarson, T. and S. Self (2003), Atmospheric and environmental effects of the 1783-1784 Laki eruption: A review and reassessment, *J. Geophys. Res.*, *1108*(D1), 4011, doi:10.1029/2001JD002042.

Trenberth, K. E., and A. Dai (2007), Effects of Mount Pinatubo volcanic eruption on the hydrological cycle as an analog of geoengineering, *Geophys. Res. Lett.*, *34*, L15702, doi:10.1029/2007GL030524.

Tukiainen, S., S. Hassinen, A. Seppala, H. Auvinen, E. Kyrola, J. Tamminen, C. Haley, N. Lloyd, and P. Verronen (2008), Description and validation of a limb scatter retrieval method for Odin/OSIRIS, *J. Geophys. Res*., 113, D04,308, doi:10.1029/2007JD008591.

Yang, K., X. Liu, P. K. Bhartia, N. A. Krotkov, S. A. Carn, A. J. Krueger, E. Hughes, and R. J. D. Spurr (2010), Direct retrieval of sulfur dioxide amount and altitude from spaceborne hyper-spectral UV measurements: Theory and application, *J. Geophys. Res.*, submitted.

Table 1. Peak values and peak Northern Hemisphere average values for total sulfate mid-visible aerosol optical depth for some recent volcanic eruptions. Values for Laki, Katmai, and Pinatubo are from *Oman et al.* [2006a]. All values are obtained from climate model simulations using ModelE.

Volcanic eruption	**Year of eruption**	**Maximum point value (no spatial averaging) of stratospheric sulfate aerosol optical depth**	**Maximum value of stratospheric sulfate aerosol optical depth when averaged over the Northern Hemisphere**
Laki	1783	1.40	0.50
Katmai	1912	0.27	0.09
Pinatubo	1991	0.30	0.14
Kasatochi	2008	0.10	0.02

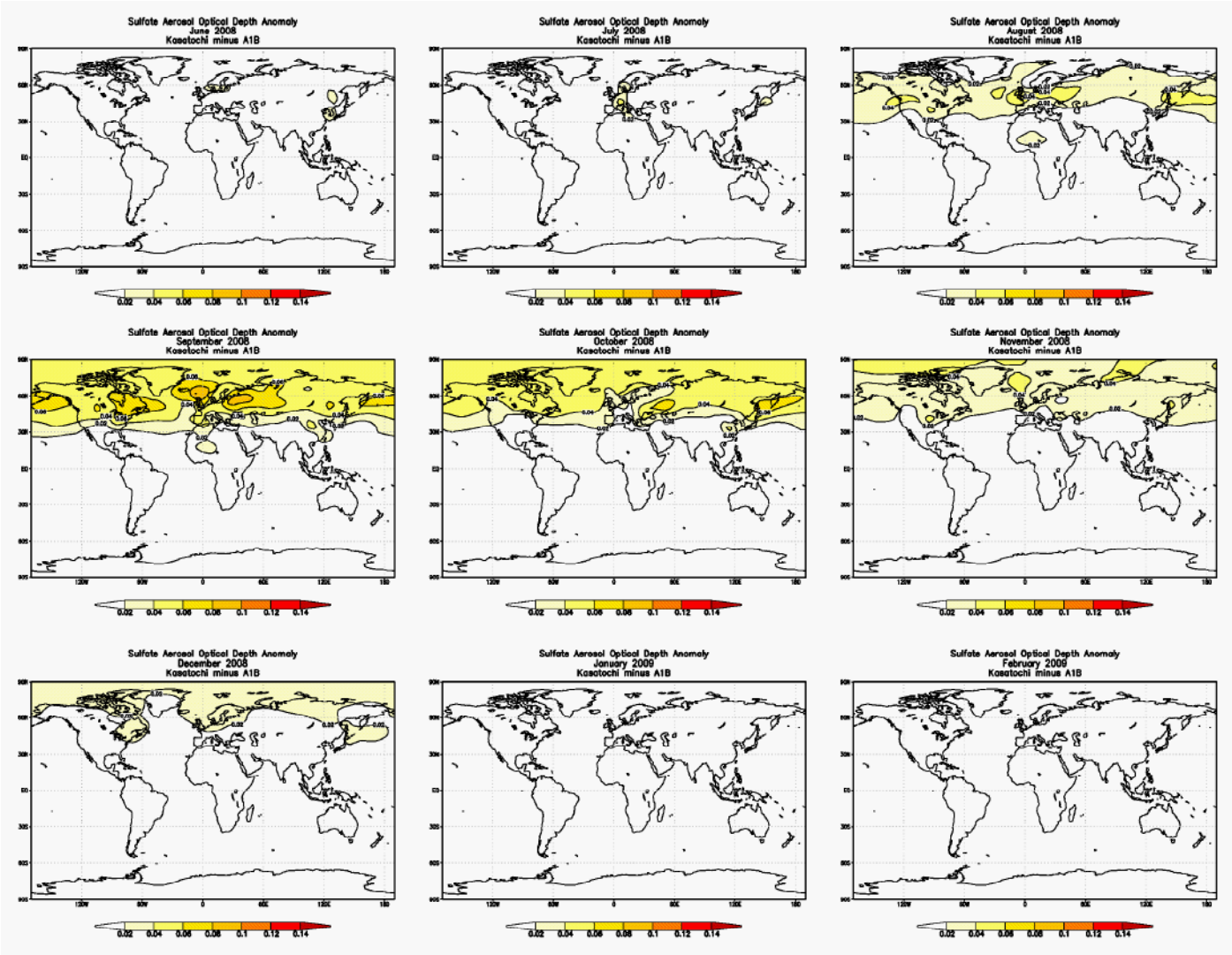

Figure 1. Time progression of anomaly in stratospheric sulfate aerosol mid-visible optical depth for the Okmok and Kasatochi volcanic eruptions from June, 2008 to February, 2009. Both the volcano ensemble and the baseline ensemble are averages of 20 runs. By February, 2009, all volcanic aerosols remaining in the atmosphere are below measurable levels.

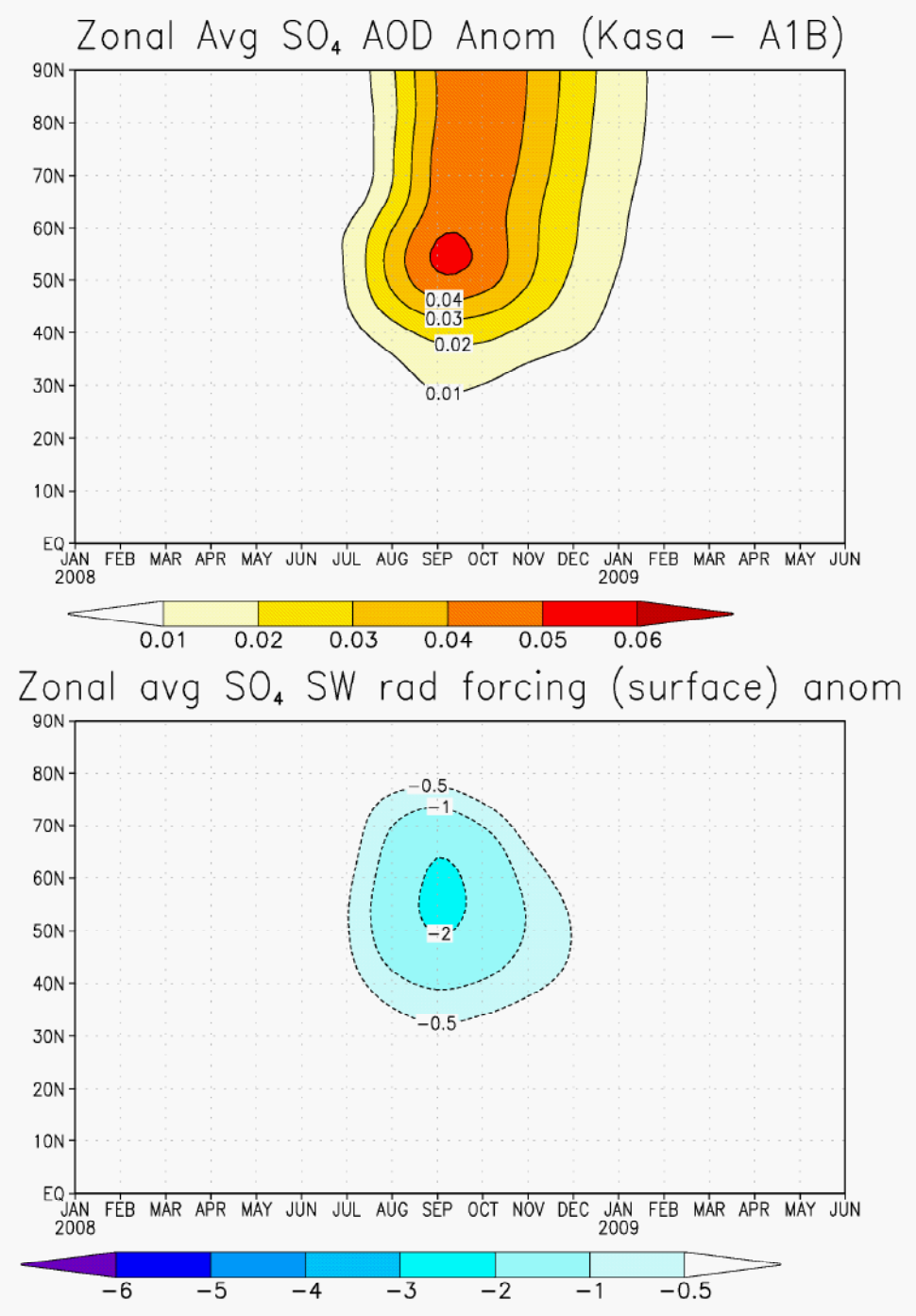

Figure 2. Zonally averaged anomalies in stratospheric sulfate aerosol mid-visible optical depth compared with zonally averaged anomalies in clear sky shortwave radiative forcing (W m^{-2}) at the surface due to sulfate aerosols. Only the Northern Hemisphere values are plotted, as the Southern Hemisphere values are zero. Results shown are for the experiment simulating the Okmok and Kasatochi volcanic eruptions. Both the volcano ensemble and the baseline ensembles are averages of 20 runs. Results shown here are similar to those in Figure 1, i.e., most of the sulfate aerosols have been deposited out of the atmosphere by February, 2009. Radiative forcing due to the sulfate aerosols ceases to be detectable even sooner.

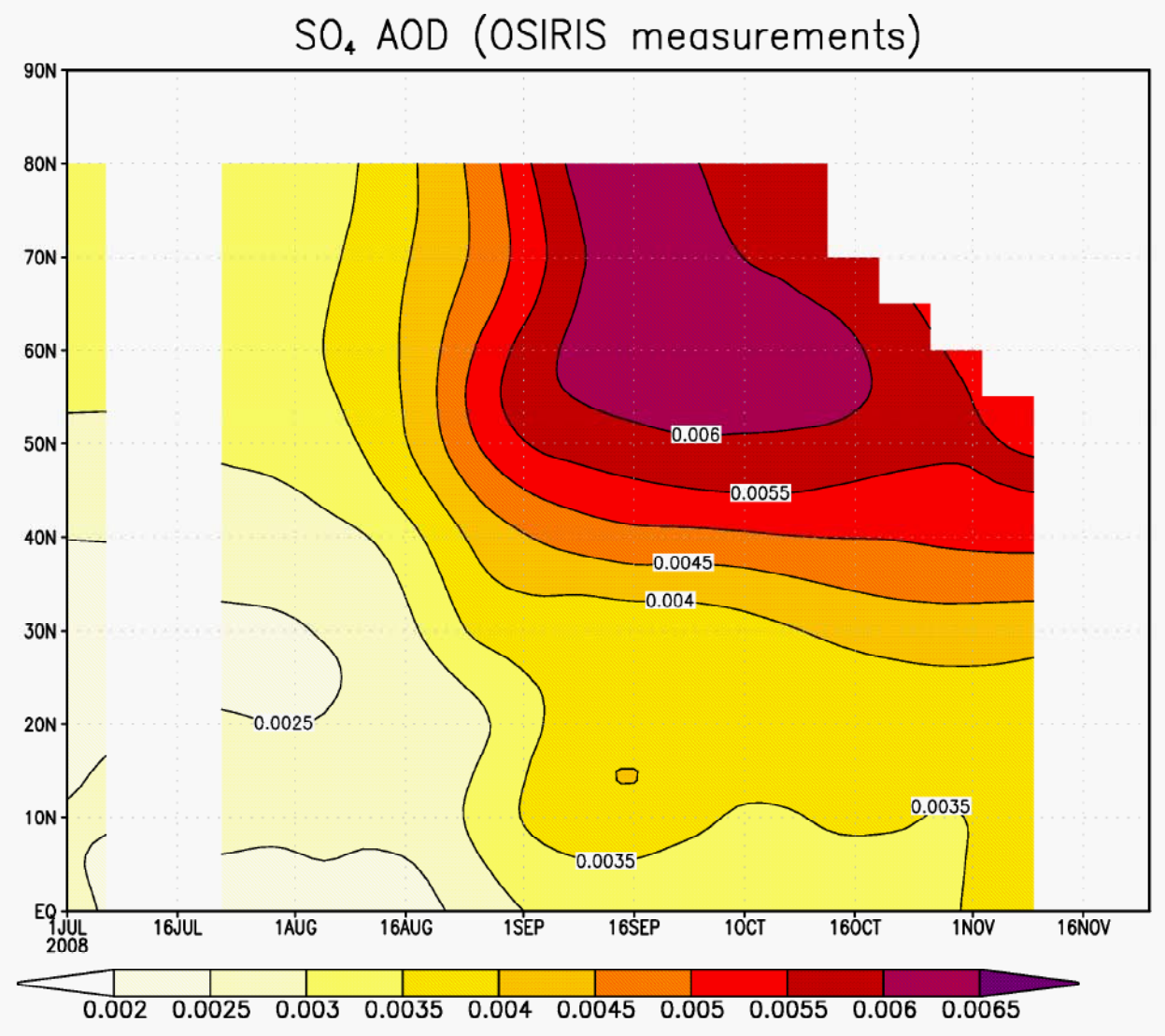

Figure 3. Zonally averaged total stratospheric aerosol optical depth measured by OSIRIS at 750 nm. Values pictured are zonal averages and are temporally averaged over 7 days. For these measurements, the vertical column extends only from the tropopause to 40 km altitude, where the tropopause is defined as altitude where the potential temperature is 380 K. OSIRIS coverage of the Northern Hemisphere extends until November.

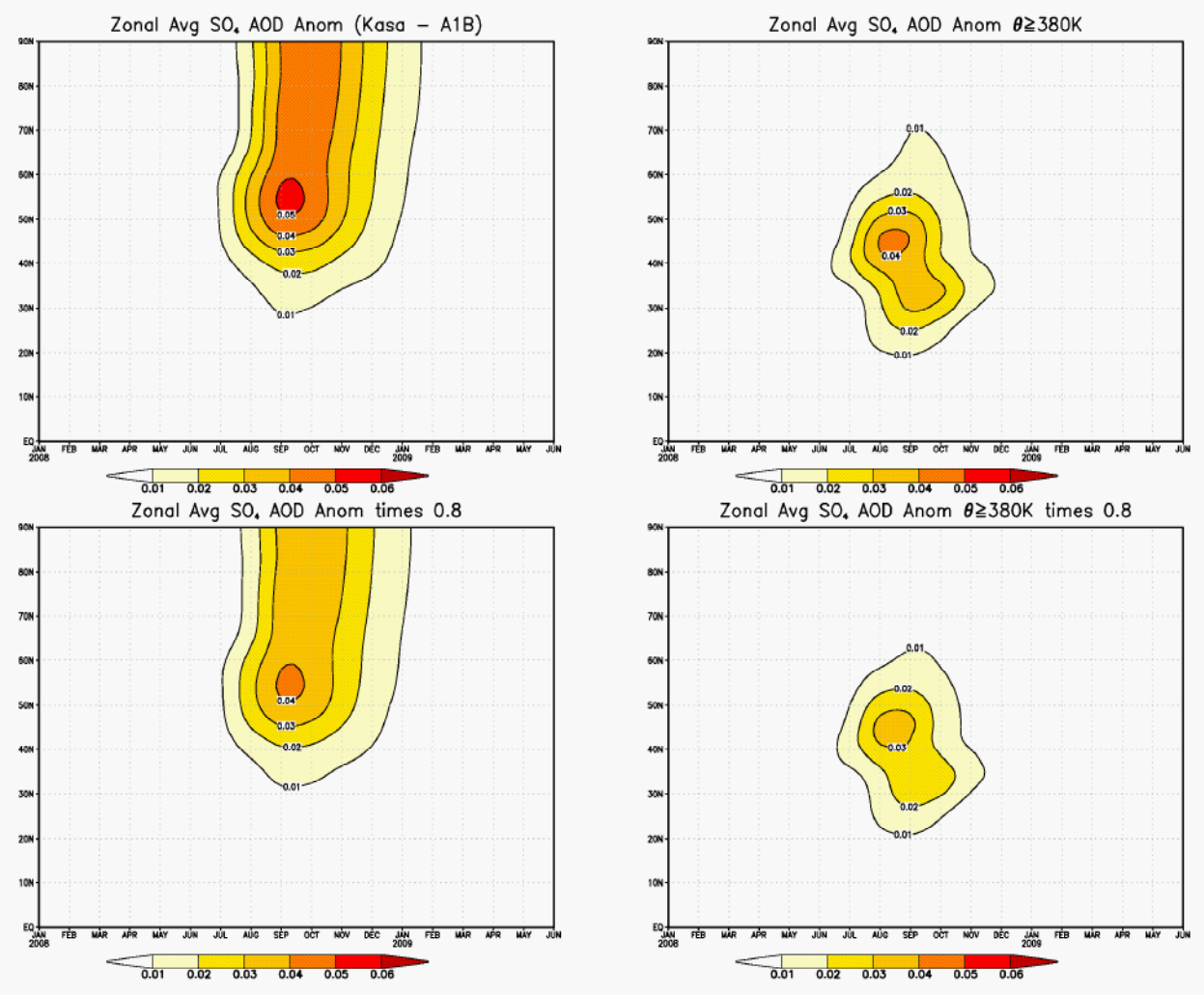

Figure 4. Zonally averaged total stratospheric aerosol optical depth anomaly as calculated by the model. Top left shows anomaly in zonally averaged optical depth. Bottom left shows the same field multiplied by 0.8 to reflect the difference in measured optical depth due to a change in wavelength. Top right shows the original field, scaled to reflect using the θ = 380 K line as the tropopause instead of the thermal tropopause. Bottom right shows a combination of both effects.

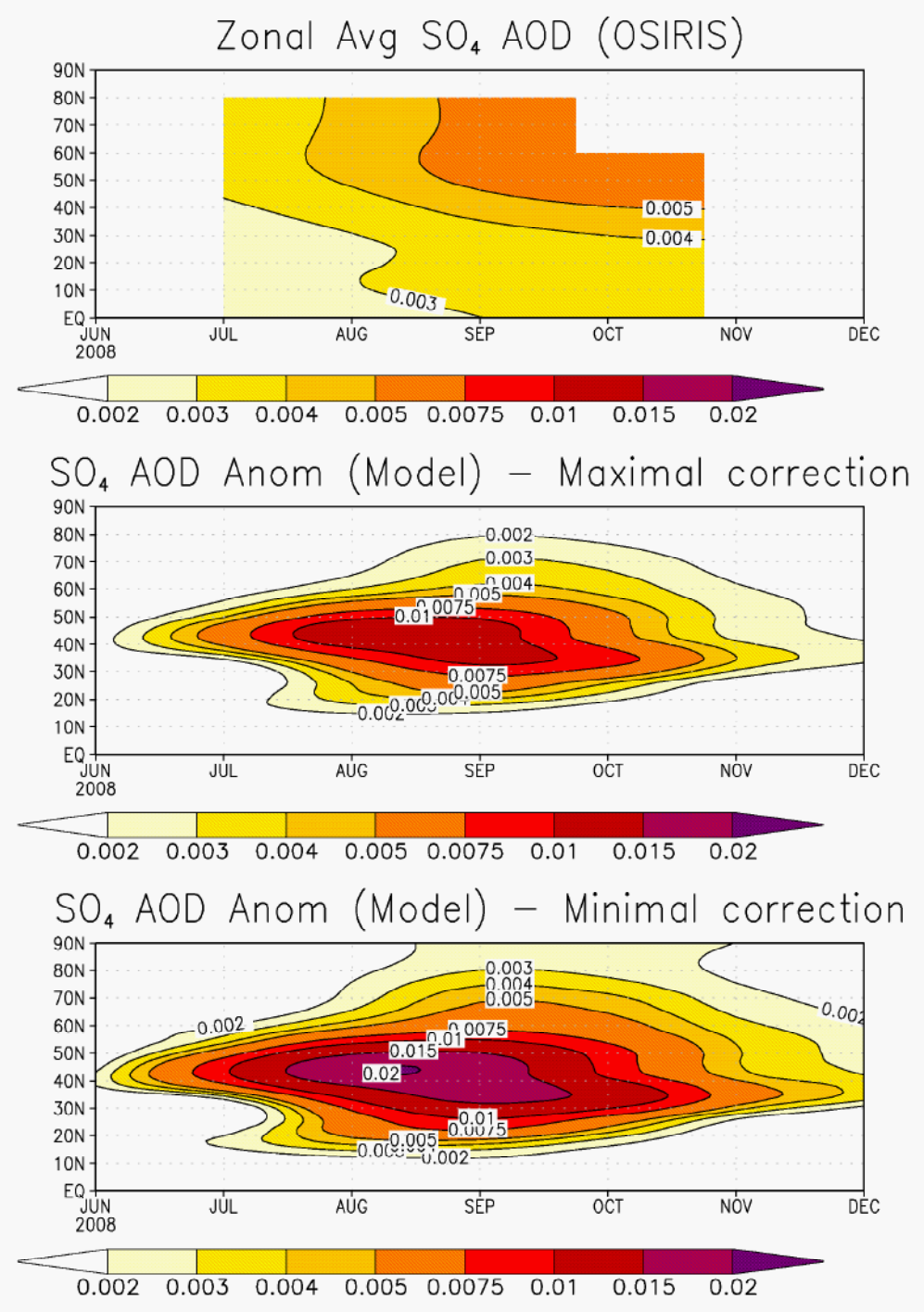

Figure 5. Zonally averaged total stratospheric aerosol optical depth comparison between the model and OSIRIS from June to December, 2008. Top panel is the results from OSIRIS but rescaled and showing monthly averages (instead of weekly as in Figure 3). Peak values in this panel may be slightly lower than in Figure 3 due to temporal smoothing. The middle panel shows the model results if the maximum amount of explainable discrepancy is taken into account. The bottom panel shows the model results if the minimum amount of explainable discrepancy is taken into account.

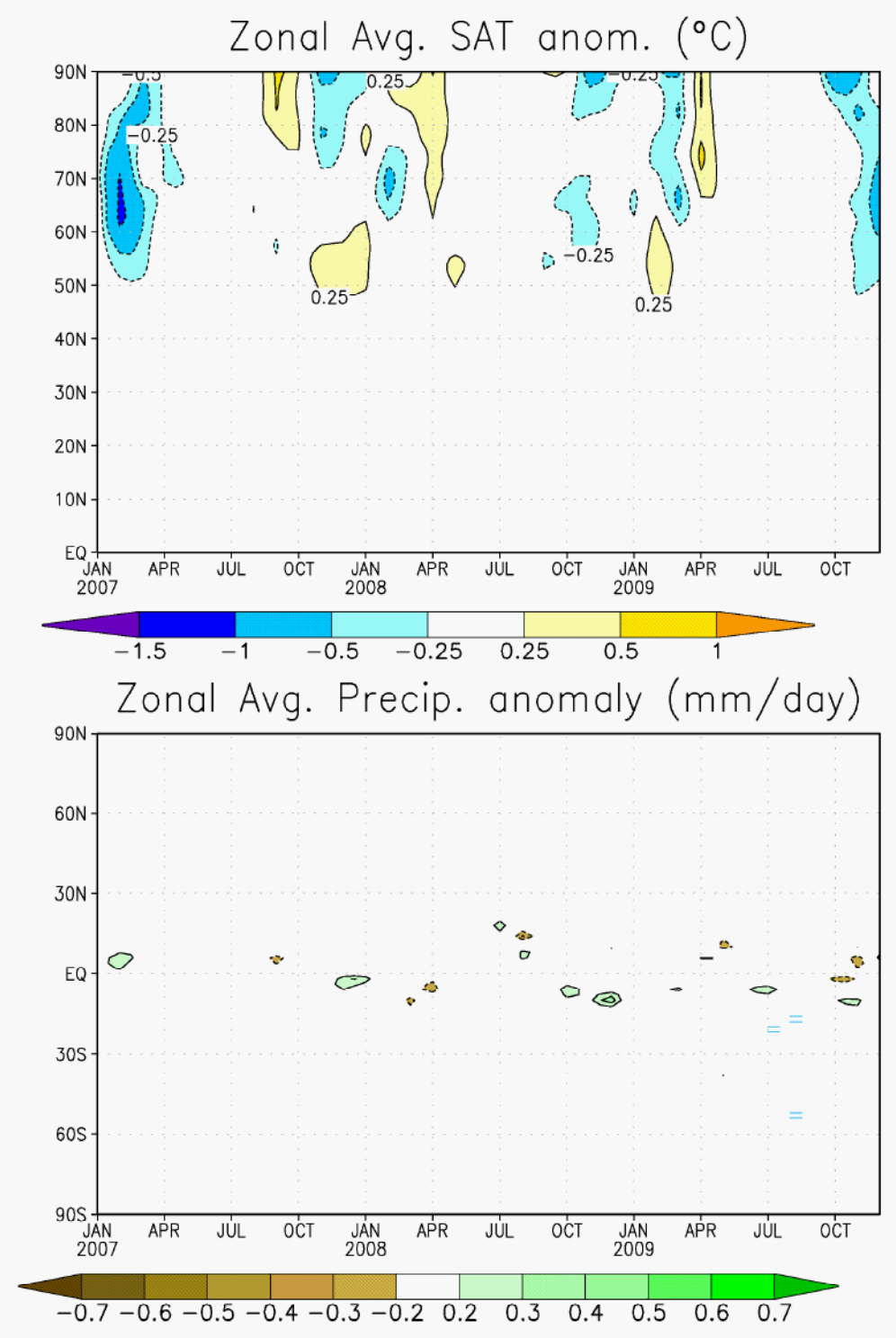

Figure 6. Zonally averaged anomalies in surface air temperature and precipitation for the Okmok and Kasatochi volcanic eruptions. The volcano ensemble and the baseline ensemble are averages of 20 runs. Only Northern Hemisphere values are pictured in the top panel since all Southern Hemisphere values are zero. Values that are statistically significant at a 95% confidence level are denoted by blue hatching.

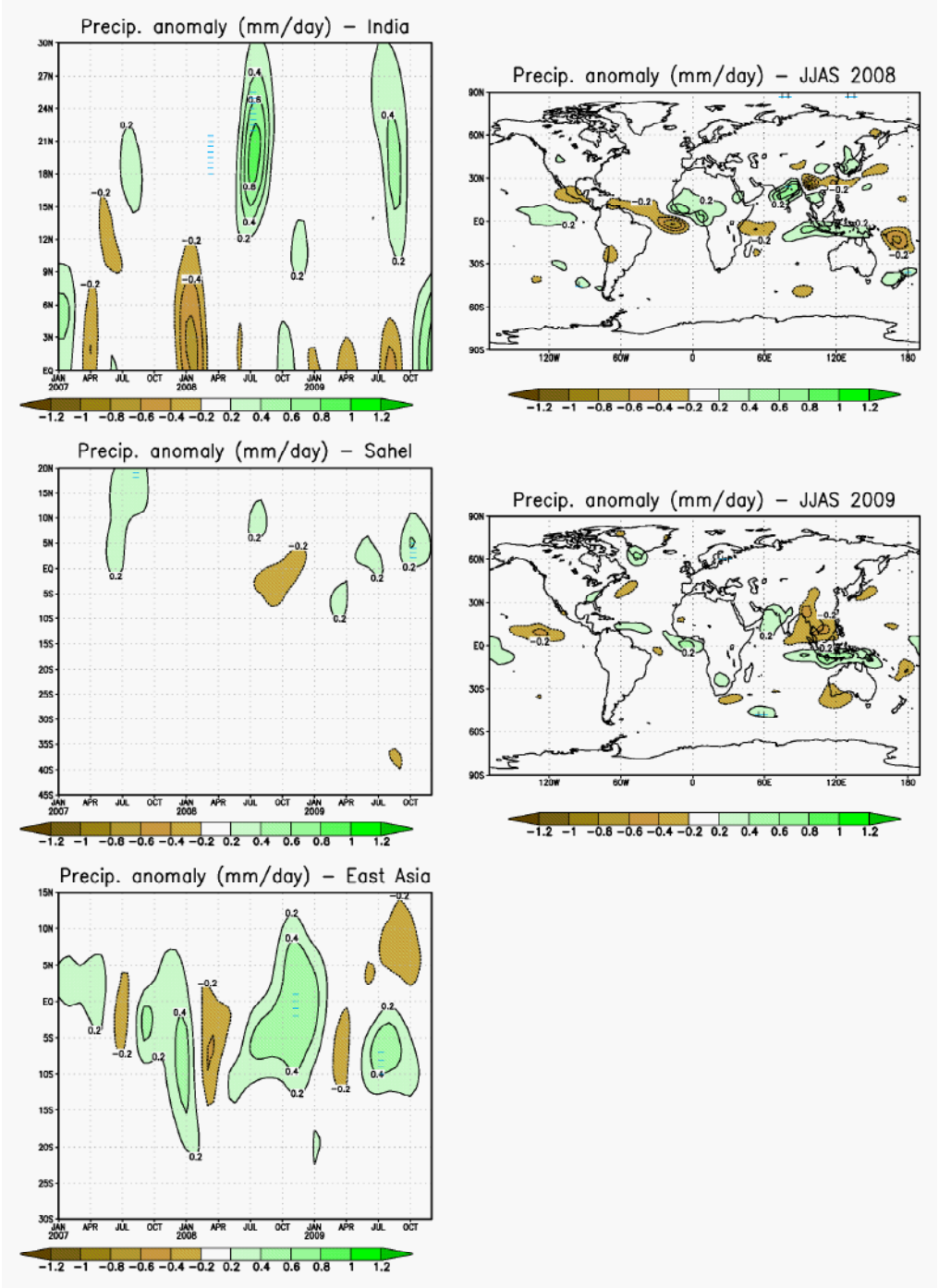

Figure 7. This figure shows monsoonal precipitation for various spatial regions and time periods. The top left shows precipitation averaged over longitudes 60°E to 90°E, highlighting the region of the Indian summer monsoon. The middle left shows precipitation averaged over longitudes 30°W to 60°E, highlighting the Sahel region. The bottom left shows precipitation averaged over longitudes 90°E to 150°E, highlighting the region of the East Asian summer monsoon. The top right shows an average of precipitation for the summer monsoon months (JJAS) in 2008, and the bottom right is for 2009. Values that are statistically significant at a 95% confidence level are denoted by blue hatching.

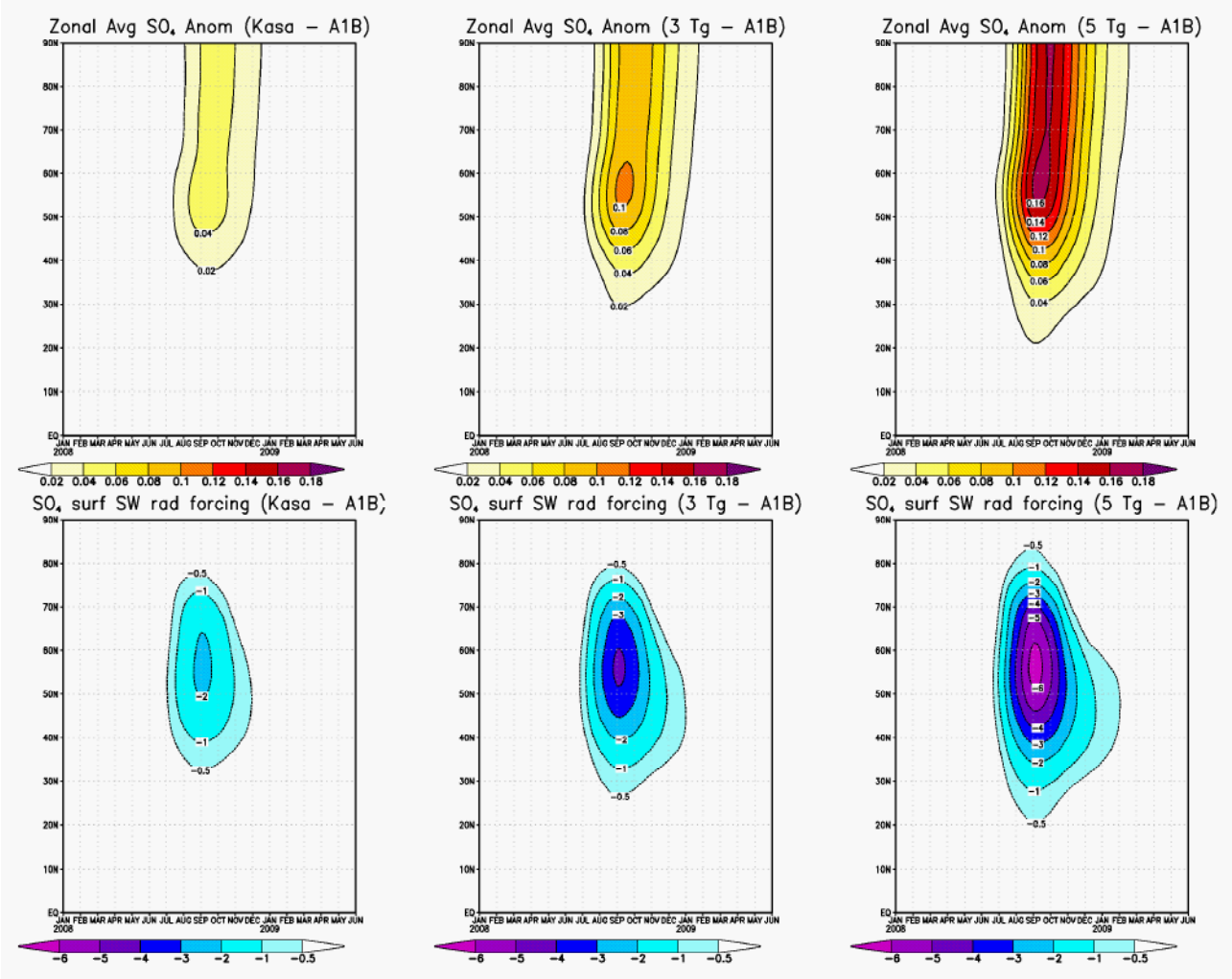

Figure 8. Comparison of zonally averaged total sulfate aerosol mid-visible optical depth and resulting anomaly in clear sky shortwave radiative forcing at the surface due to sulfate aerosols for the Okmok/Kasatochi eruption experiment, the 3 Tg SO_2 experiment, and the 5 Tg SO_2 experiment. All three volcano ensembles and the baseline ensemble are averages of 20 runs. Both aerosol optical depth and shortwave radiative forcing increase linearly with atmospheric loading of SO_2. Values in the Southern Hemisphere are zero and hence are not pictured.